Electronically Tunable Oscillator Utilizing Reinforced Controllable Parameters

LANGHAMMER, L.; ŠOTNER, R.; DOMANSKÝ, O.

Proceedings of the 2019 11th International Congress on Ultra Modern Telecommunications and Control Systems and Workshops (ICUMT), pp. 1-5

eISBN: 978-1-7281-5763-4

ISSN: 2157-023X

DOI: https://doi.org/10.1109/ICUMT48472.2019.8970997

Accepted manuscript

Electronically Tunable Oscillator Utilizing Reinforced Controllable Parameters

Lukas Langhammer, Roman Sotner, Ondrej Domansky
Faculty of Electrical Engineering and Communication
Brno University of Technology
Technicka 12, 61600 Brno, Czech Republic
xlangh01@stud.feec.vutbr.cz

***Abstract*—This paper presents a novel solution of an oscillator with electronically adjustable oscillation condition (CO) and frequency of oscillations (FO). Oscillation condition is controlled by current gain and frequency of oscillations is adjustable by transconductance and intrinsic resistance of used active elements. Both CO and FO are mutually independent. Moreover, special feature of CO allows boosting parameter driving FO (transconductance) and then shifting the whole FO range to higher bands. It allows to keep values of passive elements (capacitors especially) in satisfactory range even for higher value of FO. Simulations in PSpice confirms this hypothesis.**

Keywords—adjustable current gain, electronic control, intrinsic resistance, oscillator, transconductance

I. Introduction

The ability of controllable condition of oscillation (CO) and frequency of oscillation (FO) are very important features of many current oscillator designs and topologies [1]. The practically useful adjustment of CO and FO supposes existence of two independent parameters of the characteristic equation [1]. It means that CO and FO are settable without disturbance of each other. The first group of circuit solutions targets on values of passive elements (see [1]-[3] and references cited therein). This type of oscillators is frequently called as single resistance-controlled oscillator (SRCO) [4]. The second group covers oscillators offering ability of the electronic control of their CO and FO thanks to the usage of electronically controllable active elements (see for example [1], [5]-[11] and references cited therein). The widespread method consists in transconductance (g_m - conversion constant between voltage and current) control of FO and CO [1], [5], [6]. Other possible way of driving utilizes an intrinsic resistance of current input terminals R_X for the adjustability [1]. Methods presented in [7]-[9] combine both above-mentioned parameters in order to achieve electronic controllability of FO and CO. An example of an oscillator using current gain B to control FO can be found in [10]. A tunability implementing voltage gain A is presented in [11].

II. State-of-the-Art

The tunability of a controllable oscillator supposes existence of active elements with electronically adjustable parameters [1]. High number of solutions employs g_m of the operational transconductance amplifier (OTA) [12], [13] for these purposes. OTAs are parts of many advanced active elements [1], [7]-[9], [12].

Unfortunately, available ranges of g_m value are not favorable in modern CMOS processes (from units to hundreds of μS) [13]. Then, the design for higher operational frequencies (above 1 MHz) considers also low values of passive elements (resistors and capacitors) as well as high values of g_m. It brings significant problems with parasitic properties of the real circuit because values of elements are near to parasitic capacitances (units of pF) in high-impedance nodes [14]. Therefore, their impact on the expected value and accuracy of frequency of oscillations has really significant impact (deviations in tens of percent) and cannot be neglected.

A method how to surpass unsuitable ranges of g_m-s in the OTA is presented in this paper. It utilizes a topological feature of newly proposed circuit where a term of the numerator of the equation for oscillation frequency is reinforced (boosted) by an additional multiplicative factor. The equation for FO includes g_m parameters in standard case [5], [6]. However, our improvement consists in presence of an additional parameter. This parameter represents integer value of the current gain that can be easily increased by additional output mirrors of CMOS structure. Note that condition of oscillation is not disrupted. Despite its presence also in CO, the value is fixed in the operation because CO can be driven by the different current gain, not influencing FO. Thus, the parameter works only as multiplicative constant established at the start of the design process. It yields shift of the FO range to higher frequencies whereas range of g_m remains unchanged. We tested this effect by the simulation of standard macromodels of commercially available active elements. It is sufficient in order to confirm possible design methodology that can be generalized for any specific type of OTA and other active elements.

TABLE I. Comparison of Linearly Tunable Oscillators (Phase Shift π/4)

Reference	No of passive /active elements	Range of tunability	Used values of C	f_{0_max}/f_{0_min}	FO reinforcement implemented
[15]	4/1	1.3→7.39 MHz	30 pF	5.7:1	No
[16]	2/2	0.4→1.8 MHz	100 pF	4.5:1	No
[17]	2/3	1.1→3.3 MHz	68 pF	3:1	No
[18]	2/1	0.15→1.9 MHz	100 pF	13:1	No
This work	3/4	0.21→2.02[a] MHz	72 pF	9.6:1	No
This work	3/4	0.21→2.07[b] MHz	102 pF	9.9:1	Yes
This work	3/4	0.21→2.09[c] MHz	125 pF	10:1	Yes

[a] ideal range 0.22→2.21 MHz with 72 pF capacitors

[b] ideal range 0.21→2.21 MHz with 102 pF capacitors for FO reinforcement

[c] ideal range 0.21→2.21 MHz with 125 pF capacitors for FO reinforcement

Research described in the paper was supported by Czech Science Foundation project under No. 19-22248S.

The proposed circuitry generates two waveforms having π/4 phase shift. The selected solutions concerning similar types of the oscillator [15]-[18] are compared in Table I. None of the previously presented topologies provides the feature of the reinforcement of FO.

III. Oscillator Proposal

The proposed structure (Fig. 1) comprises one voltage differencing current conveyor (VDCC) [15], two current-mode multipliers implemented by EL2082 devices [19], single resistor, two voltage buffers and two capacitors. The internal structure of the VDCC element is depicted in Fig. 2. It was implemented by three types of commercially available active elements: LT1228 device [20] realizing the function of an operational transconductance amplifier (OTA) [12], [13]. It follows the relationship $i_{OUT} = g_m(v_{IN+}\text{-}v_{IN-})$. The second type of element is a current feedback operational amplifier (CFOA) [1], [12] implemented by AD844 device [21]. This active element can be described by the relation $i_{OUT} = i_{IN}$. The remaining active element in the VDCC structure is a current-mode multiplier (CM) realized by EL4083 [22] device. The behavior of the current multiplier (EL4083 and EL2082 devices) is characterized by $i_{OUT\pm} = \pm B i_{IN}$.

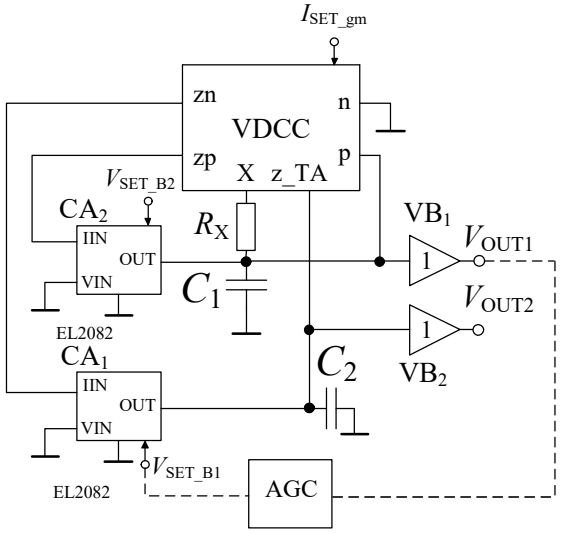

Fig. 1. Circuit diagram of the proposed oscillator.

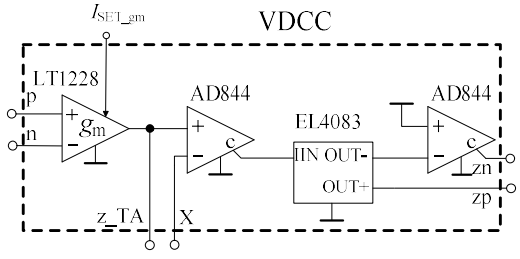

Fig. 2. CG-VDCC element realization using commercially available devices

The characteristic equation of the oscillator takes form:

$$s^2 + s\frac{C_2 + B_1C_1 - B_2C_2}{R_XC_1C_2} + \frac{g_m(B_2 - 1)}{R_XC_1C_2} = 0. \qquad (1)$$

The relations for the condition of oscillations and frequency of oscillations are given as:

$$B_2 \geq B_1\frac{C_1}{C_2} + 1,\ B_1 \leq B_2\frac{C_2}{C_1} - \frac{C_2}{C_1}, \qquad (2), (3)$$

$$f_0 = \frac{1}{2\pi}\sqrt{\frac{g_m(B_2 - 1)}{C_1C_2R_X}}. \qquad (4)$$

Based on discussion of (2), (3) and (4), CO can be controlled electronically by current gain B_1 (B_2 = constant), when FO can be also electronically tuned solely by the transconductance g_m (nonlinear control of f_0 – controlling parameter is under the root), solely by the intrinsic resistance R_X (nonlinear control of f_0), or by both parameters simultaneously when the following condition $g_m = 1/R_X$ (linear control of f_0 – can be extracted from the root since $g_m = 1/R_X$) is fulfilled. Note that B_2 can be used for boosting of g_m value that causes an increase of FO without modification of the OTA maximal available g_m value. It is useful because g_m values in modern CMOS technologies are quite limited in general (hundreds of μS).

The CO can be simplified if the values of capacitors C_1 and C_2 are supposed being equal. CO turns into: $B_2 \geq B_1 + 1$, $B_1 \leq B_2 - 1$. The initial design supposes that B_2 is set to the intended value ($B_2 = 2$) and then it must remain fixed during the further operation (in order to avoid the disturbance of FO).

The ratio of amplitudes between outputs V_{OUT1} and V_{OUT2} is:

$$\frac{V_{OUT1}}{V_{OUT2}} = \frac{1 - B_2}{1 - B_2 + sC_1R_X}. \qquad (5)$$

If we suppose equality of both capacitors $C_1 = C_2 = C$, then the ratio of amplitudes between outputs is obtained as:

$$\frac{V_{OUT1}}{V_{OUT2}} = \frac{1 + j\sqrt{g_mR_X}}{\sqrt{g_mR_X} + 1}. \qquad (6)$$

The phase shift between outputs ($\sqrt{(g_m \cdot R_X)} = 1$) achieves:

$$\frac{V_{OUT1}}{V_{OUT2}} = \frac{\sqrt{2}}{2}e^{\frac{\pi}{4}j}. \qquad (7)$$

Thus, the theoretical ratio of the output amplitudes is $V_{OUT2} = 1.4V_{OUT1}$ and the phase shift between outputs is 45°.

IV. Circuit Verification

The proposed oscillator was verified using PSpice simulations. The simulations were carried out using available behavioral models of used active elements. Selected simulations were included in the paper for illustrations. Values of capacitors were set to $C_1 = C_2 = C = 220$ pF. The tested range of values of g_m was from 0.1 mS to 1 mS. Similarly, intrinsic resistance R_X has been set in range from 10 kΩ to 1 kΩ. In case of the linear control of FO both these parameters were adjusted simultaneously when $R_X = 1/g_m$. Current gains were set as follows: $B_2 = 2$ (remains unchanged), $B_1 \leq 1$ (controlled electronically by automatic gain control (AGC) circuit in order to fulfill CO).

Fig. 3 shows the output responses (time domain) of outputs V_{OUT1} and V_{OUT2} for g_m = 1 mS and R_X = 1 kΩ. Then, the theoretical f_0 reaches 723 kHz. The simulation results yield 684 kHz. The theoretical range of f_0 depending on g_m values ($g_m = 0.1 \rightarrow 1$ mS, $B_2 = 2$, $B_1 \leq 1$) was from 229 kHz to 723 kHz (nonlinear control by g_m only). Values obtained from simulations yield range from 219 kHz to 684 kHz. The same behavior can be obtained for f_0 tuned by R_X value ($R_X = 10 \rightarrow 1$ kΩ).

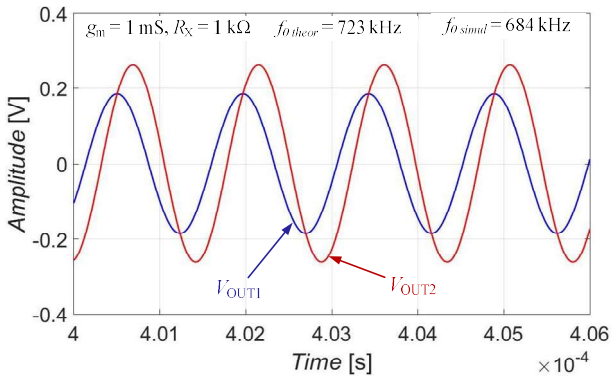

Fig. 3. Output responses of the oscillator (time domain) for $B_2 = 2$, $B_1 \leq 1$.

Fig. 4 compares the theoretical and simulated dependence of the f_0 on g_m or R_X. Both dependencies are almost identical. The differences between the theory and obtained results are getting greater as the f_0 increase especially due to the impact of parasitic capacitances in high-impedance nodes of C_1 and C_2.

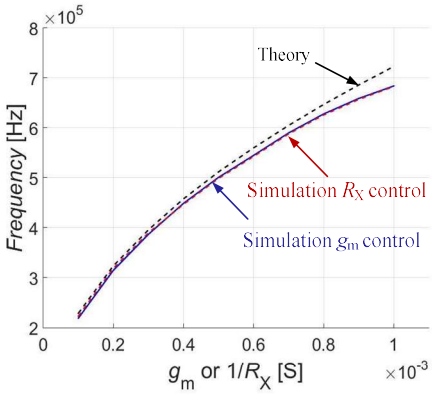

Fig. 4. Dependency of the nonlinear FO control on g_m or R_X ($B_2 = 2$).

Fig. 5 shows the linear dependence of the FO on driving parameters (simultaneously varied g_m and R_X when their ratio is $g_m = 1/R_X$) for same case as before ($B_2 = 2$, $B_1 \leq 1$). The theoretical range of obtainable f_0 in this case is from 72 kHz to 723 kHz. The simulated results provide range from 73 kHz to 684 kHz. It can be seen that the linear control of FO (when controlling g_m and R_X simultaneously) provide wider range of obtainable FO: 219 kHz to 684 kHz (f_{0_max}/f_{0_min} range of 3.2) in case of non-linear control in comparison to 73 kHz to 684 kHz (f_{0_max}/f_{0_min} range of 9.4) for the linear control.

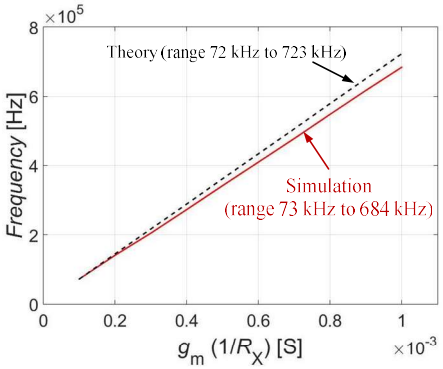

Fig. 5. Dependency of the linear FO control on used values of g_m and R_X ($g_m = 1/R_X$).

As mentioned earlier, the proposed oscillator offers a special feature of FO reinforcement (shifting the FO range to higher frequencies) thanks to its specific characteristic equation when CO and the mutual independence of CO and FO remains fulfilled. The current gain B_2 set to 3 (and $B_1 \leq 2$) modifies the relation for FO (4) to form $f_0 = 1/2\pi \cdot (2g_m/(C_1C_2R_X))^{1/2}$ whereas CO still being valid. The theoretical range of f_0 then shifts to $f_0 = 324$ kHz $\rightarrow$ 1023 kHz (nonlinear control) for $g_m = 0.1 \rightarrow 1$ mS. The simulated values fall into range 322 kHz and 923 kHz. Fig. 6 compares simulated results of standard ($B_2 = 2$, Fig. 4) and boosted ($B_2 = 3$) FO tuning range.

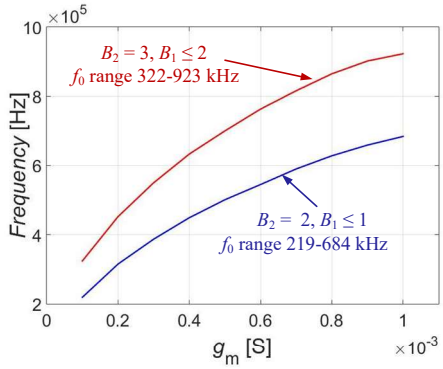

Fig. 6. Dependency of the nonlinear FO control on g_m for $B_2 = 2$ and $B_2 = 3$.

Fig. 7 illustrates the output responses (time domain) of V_{OUT1} and V_{OUT2} for values of g_m and R_X set as in Fig. 3 ($g_m = 1$ mS and $R_X = 1$ kΩ) and $B_2 = 3$ ($B_1 \leq 2$). The theoretical f_0 is equal to 1023 kHz. The obtained f_0 for outputs was 923 kHz.

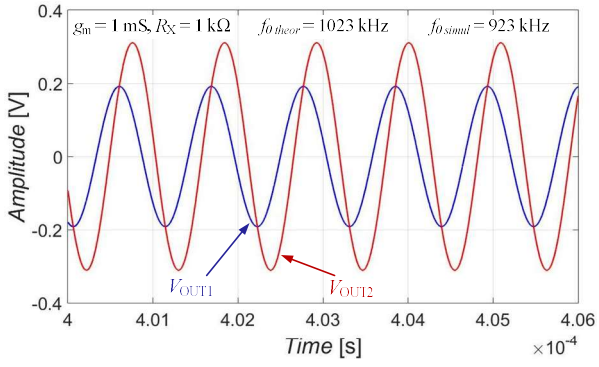

Fig. 7. Output responses of the oscillator (time domain) for $B_2 = 3$, $B_1 \leq 2$.

Comparison of the dependence of FO on the values of g_m and R_X ($R_X = 1/g_m$) for the setting $B_2 = 2$, $B_1 \leq 1$, $C_{1,2} = 72$ pF, $B_2 = 3$, $B_1 \leq 2$, $C_{1,2} = 102$ pF and $B_2 = 4$, $B_1 \leq 3$, $C_{1,2} = 125$ pF (when g_m is changed in range from 0.1 mS to 1 mS) is depicted in Fig. 8. We expect the theoretical FO tunability from 221 kHz to 2.21 MHz in all three cases ($B_2 = 2$, $B_1 \leq 1$, $C_{1,2} = 72$ pF, $B_2 = 3$, $B_1 \leq 2$, $C_{1,2} = 102$ pF and $B_2 = 4$, $B_1 \leq 3$, $C_{1,2} = 125$ pF). The simulated frequency ranges achieve values from 211 kHz to 2.02 MHz ($B_2 = 2$, $B_1 \leq 1$, $C_{1,2} = 72$ pF), 213 kHz to 2.07 MHz ($B_2 = 3$, $B_1 \leq 2$, $C_{1,2} = 102$ pF) and 211 kHz to 2.09 MHz ($B_2 = 4$, $B_1 \leq 3$, $C_{1,2} = 125$ pF). Parasitic features of high-impedance nodes (additional capacitances of units of pF) have significant effect on all cases for high frequency corner of observed FO range. However, we can see that second case (having larger values $C_{1,2} = 102$ pF) follows theoretical expectations more precisely than the first case ($C_{1,2} = 72$ pF) and the third case ($C_{1,2} = 125$ pF) even more precisely than the both previous cases. Better results (discriminability in Fig. 8) can be obtained for higher value of B_2. Nevertheless, for the same range of parameters controlling FO tuning (g_m, R_X) all the time. On the other hand, gain values (B_2 and B_1) increase.

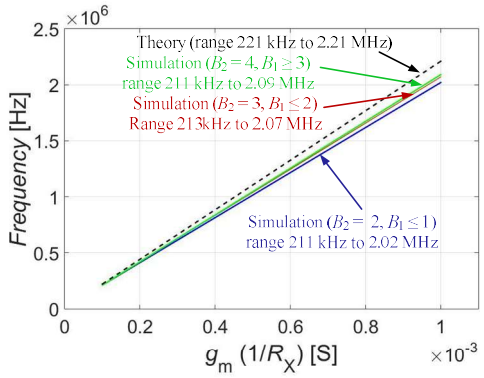

Fig. 8. Comparison of the dependency of the linear FO control for cases $B_2 = 2$, $B_1 \leq 1$, $B_2 = 3$, $B_1 \leq 2$ and $B_2 = 4$, $B_1 \leq 3$ (for $g_m = 1/R_X$).

The feature of FO reinforcement introduced in this paper could be utilized in case of other oscillator designs (as long as the circuit topology is suitable for this approach). There are some points which need to be fulfilled so the feature of reinforcement can be applied more generally to other oscillators as well: a) given oscillator provides an independent control of FO and CO (many recent proposals offer this ability). b) based on the oscillator topology and the characteristic equation of the oscillator in our case, we suppose two electronically controllable parameters (current gains B_1 and B_2 in our case), both contained in the relation for CO and one of them contained in the relation for FO. The parameter in FO (B_2 in our case) serves for shifting/boosting the FO range to higher frequencies while the other parameter (B_1) ensures that CO is fulfilled in relation to the value of B_2. The ability of the independent control of FO and CO stays fulfilled. c) these electronically controllable parameters must be able to provide a great range of the obtainable values (higher values we can get, higher values of frequencies can be obtained, or higher values of working capacitances in the topology can be used while keeping the same operational range).

Oscillators with suitable topology can benefit from the FO reinforcement feature introduced in this paper by means of possibility to use higher values of working capacitances and thus decrease the effect of parasitic characteristics, higher obtainable frequencies while allowing the values of capacitances/transconductances/resistances to stay in reasonable range, or use of easily obtainable ranges of transconductances.

V. Conclusion

The f_0 of oscillations was tested for values of g_m ($1/R_X$) from 0.1 to 1 mS providing testing range of 72 kHz → 723 kHz (for $C_{1,2} = 220$ pF). The obtained range was 73 kHz → 684 kHz. The dependence of linear and nonlinear FO control can be compared in Figs. 4, 5 and 6. The FO reinforcement allows to obtain the same available theoretical range (for g_m ($1/R_X$) = 0.1 → 1 mS) 0.221 MHz → 2.21 MHz ($B_2 = 2$, $B_1 \leq 1$, $C_{1,2} = 72$ pF) in comparison to 0.221 MHz → 2.21 MHz ($B_2 = 3$, $B_1 \leq 2$, $C_{1,2} = 102$ pF) and in comparison to 0.221 MHz → 2.21 MHz ($B_2 = 4$, $B_1 \leq 3$, $C_{1,2} = 125$ pF). The obtained ranges from simulations yield 0.211 MHz → 2.02 MHz without FO reinforcement (with $C_{1,2} = 72$ pF) and 0.221 MHz → 2.07 MHz (with $C_{1,2} = 102$ pF) and 0.221 MHz → 2.09 MHz (with $C_{1,2} = 125$ pF) with the reinforcement. Thus, the feature of FO reinforcement allows usage of capacitors of higher values when parasitic features less affect the circuit. In other words, we obtained the same (slightly improved) range of FO tuning for larger values of $C_{1,2}$ without impact on parameters intended for FO control (g_m, R_X). Similarly, the B_2 value can shift FO range to higher frequencies in case of nonlinear dependence of FO on g_m or R_X without change of $C_{1,2}$ as shown in Fig. 6. These parameters have still the same range of control in all cases. Moreover, B_2 can be set to higher values as long as condition $B_1 \leq B_2 - 1$ remains fulfilled. The verification of discussed hypothesis was the most important goal of this work.

References

[1] R. Senani, D. R. Bhaskar, V. K. Singh, R. K. Sharma, Sinusoidal Oscillators and Waveform Generators using Modern Electronic Circuit Building Blocks, Switzerland: Springer International Publishing, 2016, pp. 1–622.

[2] A. Lahiri, "Current-mode variable frequency quadrature sinusoidal oscillator using two CCs and four passive components including grounded capacitors," Analog Integr. Circuits Signal Process, vol. 68, no. 1, 2011, pp. 129–131.

[3] A. M. Soliman "On the generation of CCII and ICCII oscillators from three Op Amps oscillator," Microelectron. J., vol. 41, no. 10, 2010, pp. 680–687.

[4] V. K. Singh, R. K. Sharma, A. K. Singh, D. R. Bhaskar, R. Senani, "Two New Canonic Single-CFOA Oscillators With Single Resistor Controls," IEEE Transactions on Circuits and Systems – II: Express Briefs, vol. 52, no. 12, 2005, pp. 860–864.

[5] A. Rodriguez-Vazquez, B. Linares-Barranco, J. Huertas, E. Sanchez-Sinencio, "On the Design of Voltage-Controlled Sinusoidal Oscillators Using OTA's" IEEE Transactions on Circuits and Systems, vol. 37, no. 2, 1990, pp. 198–211.

[6] S-H. Tu, Y-S. Hwang, J-J. Chen, A. M. Soliman, C-M. Chang, "OTA-C arbitrary-phase-shift oscillators", IEEE Transactions on Instrumentation and Measurement, vol. 61, no. 8, 2012, pp. 2305–2319.

[7] W. Jaikla, M. Siripruchyanun, A. Lahiri, "Resistorless dual-mode quadrature sinusoidal oscillator using a single active building block," Microelectron. J., vol. 42, no. 1, 2011, pp. 135–140.

[8] W. Jaikla and P. Prommee, "Electronically tunable current-mode multiphase sinusoidal oscillator employing CCCDTA-based allpass

filters with only grounded passive elements," Radioengineering, vol. 20, no. 3, 2011, pp. 594–599.

[9] Y. Li, "Systematic derivation for quadrature oscillators using CCCCTAs," Radioengineering, vol. 24, no. 2, 2015, pp. 535–543.

[10] D. Biolek, A. Lahiri, W. Jaikla, M. Siripruchyanun, and J. Bajer, "Realization of electronically tunable voltage-mode/current-mode quadrature sinusoidal oscillator using ZC-CG-CDBA," Microelectron. J., vol. 42, no. 10, 2011, pp. 1116–1123.

[11] R. Sotner, J. Jerabek, N. Herencsar, J.-W. Horng, K. Vrba, and T. Dostal, "Simple oscillator with enlarged tunability range based on ECCII and VGA utilizing commercially available analog multiplier," Measurement Science Review, vol. 16, no. 2, 2016, pp. 35–41.

[12] D. Biolek, R. Senani, V. Biolkova, Z. Kolka, "Active Elements for Analog Signal Processing: Classification, Review, and New Proposals," Radioengineering, vol. 17, no. 4, 2008, pp. 15–32.

[13] E. Sanchez-Sinencio, J. Silva-Martinez, "CMOS transconductance amplifiers, architectures and active filters: a tutorial," IEE Proc. Circ. Dev. Systems, vol. 147, no. 1, 2000, pp. 3–12.

[14] R. Sotner, J. Jerabek, N. Herencsar, J. Petrzela, "Methods for Extended Tunability in Quadrature Oscillators Based on Enhanced Electronic Control of Time Constants," IEEE Transactions on Instrument. and Measurement, vol. 67, no. 6, 2018, pp. 1495-1505.

[15] R. Sotner, J. Jerabek, J. Petrzela, N. Herencsar, R. Prokop, K. Vrba, "Second-Order Simple Multiphase Oscillator Using Z-Copy Controlled-Gain Voltage Differencing Current Conveyor" Elektronika Ir Elektrotechnika, vol. 20, no. 9, 2014, pp. 13–18.

[16] R. Sotner, J. Jerabek, N. Herencsar, J. Horng, K. Vrba, "Electronically Linearly Voltage Controlled Second-Order Harmonic Oscillator With Multiples of pi/ 4 Phase Shifts," In Proc. of the 38th International Conference on Telecommunication and Signal Processing, Berlin, Germany, 2014. pp. 708–712.

[17] R. Sotner, J. Jerabek, N. Herencsar, K. Vrba, T Dostal, "Features of multi-loop structures with OTAs and adjustable current amplifier for second-order multiphase/quadrature oscillators," AEU - International Journal of Electronics and Communications, vol, 69, 2015, pp. 814–822.

[18] R. Sotner, J. Jerabek, N. Herencsar, K. Vrba, "Design of the simple oscillator with linear tuning and pi/4 phase shift based on emulator of the modified current differencing unit." IEICE Electronics Express, vol. 12, no. 19, 2015, pp. 1–7.

[19] Intersil (Elantec), EL2082 CN Current-mode multiplier (datasheet), 1996, accessible on www: http://www.intersil.com/data/fn/fn7152.pdf.

[20] Linear Technology, LT1228 Current Feedback Amplifier with DC Gain Control (datasheet), accessible on http://cds.linear.com/docs/en/datasheet/1228fd.pdf.

[21] Analog Devices, AD844 Operational Amplifier (datasheet), 1989, accessible on http://www.analog.com/media/en/technical-documentation/data-sheets/AD844.pdf.

[22] Intersil (Elantec), EL4083 CN Current-mode multiplier (datasheet), 1996, accessible on www.intersil.com/content/dam/Intersil/documents/el40/el4083.pdf